



NIH Public Access

Author Manuscript

J Phys Chem B. Author manuscript; available in PMC 2009 February 21.

Published in final edited form as:

J Phys Chem B. 2008 December 4; 112(48): 15442–15449. doi:10.1021/jp804965x.

Interaction between Glycine/ Glycine Radicals and Intrinsic/Boron-doped (8, 0) Single-walled Carbon Nanotubes: A Density Functional Theory Study

Wenming Sun[†] and Yuxiang Bu^{*,†}

The Center for Modeling & Simulation Chemistry, Institute of Theoretical Chemistry, Shandong University, Jinan, 250100, P.R. China

Yixuan Wang[‡]

Department of Natural Science, Albany State University, Albany, Georgia 31705

Abstract

The adsorptions of a glycine molecule as well as dehydrogenated radicals on the side walls of both intrinsic and boron-doped (B-doped) single-walled (8,0) carbon nanotubes (SWCNTs) were investigated by a density functional theory. A glycine molecule tends to physically adsorb on intrinsic SWCNT, yet chemically adsorb on B-doped SWCNT as a result of a somewhat chemical bond between the electron-rich nitrogen atom of the glycine molecule and the electron-scarce boron atom of the doped SWCNT. Opposite to the previous report (*J. Phys. Chem. B* **2006**, *110*, 6048-6050), it is found in the present study that both the N-centered and C-centered glycine radicals can form quite stable complexes with intrinsic as well as B-doped (8, 0) SWCNTs. When the B-doped SWCNT interacts with glycine radicals, although there is a competition between B and the neighbor C in the nanotube axis direction, glycine radicals preferentially bind to the C site. The encapsulations of a glycine molecule into SWCNTs with various diameters are also discussed. We find that the encapsulation process is endothermic for (8, 0) and (9, 0) SWCNTs, while it is exothermic for (10,0) SWCNT, indicating that the critical diameter of the zigzag SWCNT for the encapsulation is 7.83 Å, the diameter of (10,0).

1. Introduction

Since their discovery in 1991,¹ carbon nanotubes (CNTs) have attracted considerable interests in the field of nanotechnology due to their unique properties. Their high electrical conductivity and strength have made them promising materials for new applications such as field emitters^{2,3} and scanning probes.⁴ Besides their electronic and mechanic applications, there are some reports about their applications in bio-technology⁵⁻⁹ and molecular sensors.¹⁰⁻¹² The immobilization of oligonucleotides and proteins can be carried out via either encapsulating

Correspondence to: Yixuan Wang.

*The corresponding authors: Yuxiang Bu, e-mail: byx@sdu.edu.cn; Yixuan Wang, e-mail: Yixuan.Wang@asurams.edu.

[†]Shandong University

[‡]Albany State University

Supporting Information Available: Figure S1 displays the optimized structures of triplet state complexes for N-centered and C-centered radicals with B-(8,0) CNT. The HOMO and LUMO of CNT cluster C64H16 are illustrated in Figure S2. Table S1 summarizes the geometry parameters of glycine molecule and radical isomers. Table S2 lists the total energies and bonding energies for the singlet and triplet complexes arising from N- and C-centered radicals with B-(8,0) CNT. This material is available free of charge via the Internet at <http://pubs.acs.org>.

into or wrapping around nanotubes without losing their activity and immunological properties.
13-16

Amino acids are the elementary units for composing biomolecules and can also reflect the common chemical properties of complicated biomolecules. The interaction between SWCNTs and typical amino acids is therefore very important for understanding the interaction mechanism between SWCNTs and biomolecules. The small size of glycine allows exhaustive study on its interaction with a surface of CNT at reasonable computational cost. Insights into interaction between glycine and SWCNTs may therefore give some important guidance to further study of interaction between complicated biomolecules and SWCNTs.

Despite biological interest there are few detailed theoretical investigations of the interaction between glycine and CNTs. One recent publication deals with the interaction between glycine radicals and SWCNTs,⁵ yet CNT cluster models were used there to perform the calculation. When the dangling bonds at the end of tubes were saturated by H atoms, the highest-occupied molecule orbital (HOMO) distributes over C-H bonds instead of the sidewall. Thus, the absence of periodic-boundary condition could not well display effects of the electronic structures, and might give error information associated with the adsorption mechanism. To the best of our knowledge there is no report on the interactions between different glycine conformers and SWCNTs. In order to gain insight into these interactions, we choose two representative glycine conformers as shown late.

In recent years the doped CNTs with other atoms have been shown to chemically adsorb molecules such as CO, H₂O, HCOOH and HCN.¹⁷⁻¹⁹ In the present work, we are also interested in the interaction between glycine, glycine radicals with B-doped (8,0) SWCNT. In brief, the primary objective of the paper is to investigate the interaction of glycine and glycine radicals with the intrinsic (8, 0) and B-doped (8, 0) SWCNTs. The encapsulation of glycine into the intrinsic (8, 0) SWCNT will also be briefly discussed.

2. Models and Methods

The calculations are based on the density functional theory (DFT) using numerical orbital as basis sets, and were done with the Cerius² 4.6 suite of program DMol³ package from Accelrys, Inc.²⁸ Using the generalized gradient approximation (GGA) method that was parametrized by Perdew and Wang's scheme²⁰ (PW91) with a double numerical plus polarization function (DNP), full geometry optimizations and property calculations were performed for the intrinsic and B-doped (8,0) SWCNT systems with and without glycine molecules. Periodic-boundary condition and a super cell approximation with a lateral separation of 24 Å between the centers were used to make sure that the SWNT plus the glycine molecule would not interact with their periodic images. The super cell includes 64 atoms of the nanotube (64 carbon atoms for the intrinsic SWCNT vs 63 carbon atoms plus 1 boron atom for the B-doped SWCNT) and a glycine molecule or its radicals with a total length of 8.520 Å along the tube. The spin polarization scheme was utilized to deal with open-shell systems. Two k-points generated by Monkhorst-Pack method were used in the k-sampling, which was shown to be a good approximation for (8, 0) carbon nanotubes.²¹ The convergence threshold of energy was set as 10⁻⁵ a.u..

To evaluate the interaction between a glycine molecule or a radical and intrinsic or B-doped SWCNT, the binding energy (E_b) was calculated according to the following equation,

$$E_b = E(\text{glycine} - \text{SWCNT}) - E(\text{glycine}) - E(\text{SWCNT}) \quad (1)$$

Where $E(\text{glycine-SWCNT})$ is the total energy of the complex consisting of glycine and the (8,0) SWCNT, and $E(\text{glycine})$ and $E(\text{SWCNT})$ are the total energies of glycine and SWCNT,

respectively. Thus, the negative value of the binding energy denotes exothermic adsorption. Eq. (1) eliminates deformation energy, but basis set superposition error (BSSE) has not been included. Technically BSSE treatment is unavailable with DMol³. BSSE inclusion does reduce binding energy for dimerization by 1-2 kca/mol with DFT method and beyond double zeta basis set,³¹ but usually it will not change general conclusion, especially for the relatively strong interaction systems like the current glycine+B-(8,0), glycine radical+CNT. It is known that, in spite of great improvement over LDA, a typical GGA type of DFT like PW91 method still underestimates the binding for the systems mainly arising from van der Waals interaction, which may partially make up for the failure to include BSSE. Thus it is most likely that the present binding energies (refer to Table 1) of glycine conformers (I and II) and intrinsic (8,0) SWCNT are lower than real ones, while the other relatively strong interactions should be proper.

3. Results and Discussions

For a glycine molecule, both *trans*- (**I**) and *cis*- (**II**) conformers with respect to C-C bond in Figure 1 were chosen as models in the calculation. Trans-conformer **I** is more stable than cis-conformer **II** by approximately 3.6 kcal/mol at B3LYP/6-31G* level. Among the possible radicals in gas phase are the ones based on conformer **I** from which one hydrogen atom is abstracted either from the α -C atom (C-centered radical, **III**) or the N atom (N-centered radical, **IV**). It is found that the C-centered radical, **III** is favored over the N-centered one, **IV** by 20.2 kcal/mol at B3LYP/6-31G* level with Gaussian 03 package.²² This result is in very good agreement with the value of 19.9 kcal/mol predicted with G2(MP2).²⁹ Taking into account the different DFT, basis set and software, this result also reasonably agrees with the values of 22.7 kcal/mol predicted by BLYP/SVP with TURBOMOLE,⁵ and 18.5 kcal/mol with HF/6-31G*.³⁰ We also designed analogical radicals based on conformer **II**, but the corresponding radicals were less stable than their counterparts from conformer **I**, these conformations were therefore not discussed here. The relevant geometry parameters are summarized in Table S1.

Figure 2 shows a structural model of the (8, 0) SWCNT. The average bond length between carbon atoms of intrinsic (8, 0) SWCNT is 1.423 Å (the lengths of bonds which are parallel and slanted to the axis of tube were 1.413 and 1.434 Å, respectively), which is in good agreement with the experimental value of 1.44 reported elsewhere.²³ In the B-doped SWCNT, the lengths between B atom and the surrounding C atoms are 1.495, 1.521 and 1.521 Å, respectively. The HOMO-LUMO energy gap of intrinsic and B-doped (8, 0) SWCNT are 0.61 eV and 0.41 eV, respectively. The calculated energy gap of semiconducting (8, 0) CNT is wider than 0.56-0.58 eV.^{17, 18} The difference may mainly come from the basis sets (i.e., the numerical basis set in DMol³ and the plane-wave basis set in VASP) and the different computational codes implemented and computational parameters (e.g., the size of lattice adopted in these works). DOS graphs of intrinsic and B-doped (8, 0) SWCNT were presented in Figure 4, and a comparison indicates that after B atom was doped the gap changes significantly. The HOMOs of these two CNTs were shown in Figure 5.

3.1 The adsorption of a glycine molecule on the surfaces of intrinsic and B-doped (8, 0) SWCNTs

For the adsorptions of glycine on SWCNT, the tilted configurations are located with respective one and two hydrogen atoms of NH₂ group pointing to the center of six-membered ring of the SWCNT. Similar to cases of NH₃/CNT and cytosine/CNT,^{24,6} the configuration with one H atom downward (3a in Figure 3) is slightly more stable than that with two H atoms downward by 0.07 kcal/mol (E_b : -1.44 vs -1.37 kcal/mol). In configuration 3a, neither the glycine nor the SWCNT undergoes a significant deformation. Compared with the intrinsic SWCNT, the DOS (**a** in Figure 4) of this adsorption configuration is clear in the sense that below the Fermi level, the electronic states are modified in the regions of valence band. However, the gap does not

NIH-PA Author Manuscript NIH-PA Author Manuscript NIH-PA Author Manuscript

change at all. Mulliken charge population analysis indicates that the amount of charge transferred from glycine molecule to SWCNT is almost zero. To gain further insight into the adsorption electronic structure, the HOMO of the complex is presented in **5a**, Figure 5 from which it can be observed that conformer I has no clear contribution. Thus, it could be concluded that the glycine conformer **I** is physically adsorbed on the intrinsic (8, 0) SWCNT with a binding energy of approximately of -1.4 kcal/mol.

Conformer **II** also undergoes a physisorption process when interacts with intrinsic (8, 0) SWCNT, as shown in **3c**, Figure 3. In the complex **3c**, NH seems to be adsorbed in the C=C bridge site with H and C distances of 2.766 and 2.961 Å. The distance between H atom pointing to the ring and the center of the outermost ring of (8,0) SWCNT is 3.327 Å. The binding energy of **3c** is more negative than **3a** by 0.2 kcal/mol. A comparison of the two DOS graphs (**a** and **c** in Figure 4) shows that below the Fermi level, the electronic states slightly differ between -3.0 and -0.4 eV, and these differences may mainly attribute to the isolated glycine molecule. In the cases of the conduction band and the gap, there is no difference after adsorption, either. Likewise, the glycine conformer **II** had no contribution towards the HOMO of this system (**5c** in Figure 5).

Thus, after analyzing the structural and electronic properties of two absorption configurations (**3a** and **3c**), we can conclude that the intrinsic SWCNT only weakly binds to glycine molecule. The presence of glycine molecule would neither modify the DOSs of the SWCNT nor lead to a change in the conductivity of the SWCNT.

Oppositely, for the B-doped (8, 0) SWCNT considerable changes of properties of nanotube have been observed. **I**-B-doped SWCNT complex, **3b** illustrates a significant deformation of both glycine **I** and B-doped (8, 0) SWCNT. For glycine the bond lengths of N₁C₃, C₃C₄ and C₄O₉ are 1.477, 1.511 and 1.353 Å, respectively, which are different from those in Figure 1 (1.449, 1.522 and 1.365 Å). While for the B-doped SWCNT, the B atom bulges out of the surface of CNT, and the distances between B and C₄, C₂ and C₃ atoms are 1.552, 1.595 and 1.595 Å, respectively. The angles of N-B-C4, N-B-C2, and N-B-C3 (numbering as in Figure 2) are 109.9°, 108.5°, and 109.0°, respectively, showing that the hybridization character of B is changed from pure sp² type to somewhat sp³ type. The distance between the N atom and B atom is 1.675, longer than the bond length of N-B (1.44-1.46 Å) in BN nanotube (BNNT).²⁵ From the DOS image (**b** of Figure 4) of this configuration, it can be seen that the band gaps near Fermi level disappear, indicating that the B-doped SWCNT switches from semiconductor to conductor, and a significant conductivity increase is expected. A significant amount of charge transferred from glycine **I** to the B-doped SWCNT is 0.318e, much higher than that in the **I**-SWCNT complex, **3a**. Because of one valence electron less than C, as B replaces C atom in the surface of SWCNT the electronic structure contains an electronic hole, generating a p-type semiconductor. When it interacts with the electron-rich N atom in glycine molecule, the lone electron pair of N in glycine is transferred to the empty orbital of B atom (**5b** of Figure 5), which dramatically changes the conductance of the nanotube and made the semiconducting B-doped SWCNT more conductive.

Analogously, conformer **II** also undergoes a chemisorption when it interacted with B-doped (8, 0) SWCNT, as shown in **3d** of Figure 3. The distance from N to B atom is 1.714 Å, and the binding energy is -33.9 kcal/mol. The amount of charges transferred from glycine **II** to the B-doped SWCNT is 0.290e. Likewise, the HOMO-LUMO gap, 0.18 eV is considerably lower than the gap of 0.41 eV of B-doped (8, 0) SWCNT. Little difference could be observed by comparing the DOS graphs (**d** and **b**) of this complex (**3d**) with that of I-B-doped SWCNT (**3b**).

After analyzing the geometric structures and electronic properties of two complexes (3b and 3d) resulting from the interactions of glycine molecule isomers with B-doped (8, 0) SWCNT, the following conclusions can be reached. As B atom replaces C atom in the intrinsic SWCNT, the electronic structure contains an empty p orbital. When glycine molecules interact with the B-doped SWCNT, electron-rich N of glycine tends to somewhat chemically absorb on the B-SWCNT, which is evidenced by considerable charge transfer (0.32e in 3b and 0.29e in 3d), negatively high binding energy (-33.2 and -33.9 kcal/mol of 3b and 3d, respectively), and great contribution of glycine to HOMOs.

3.2 The adsorption of glycine radicals on the surfaces of intrinsic and B-doped (8, 0) SWCNTs

A few publications dealt with the adsorption of glycine radicals on the surfaces of CNTs. For example, Mavrandakis et al had reported interactions of glycine radicals with (8, 0) and (4, 4) CNTs using density functional theory.⁵ They found that the C-centered radical could not form a stable complex with both CNTs. However, as shown by 6e in Figure 6, both the C-centered radical and SWCNT undergo significant deformation due to their significant interaction. The C-centered radical distorts significantly, and the carbon atom at adsorption site bulges out of the tube surface. The α carbon of the glycine radical and the carbon atom of the tube surface are jointed by an almost single bond. This C-C distance (1.629 Å) is slightly larger than that between the carbon atoms in CNT and in glycine molecule, which were 1.44 and 1.52 Å, respectively. HOMO graph shows that primary contribution in glycine side comes from the alpha carbon of the C-centered glycine radical. The bond lengths of C-C in SWCNT are significantly extended to 1.499, 1.532 and 1.533 Å, respectively. It can be therefore determined that the hybridization of carbon atom changes from regular sp^2 to sp^3 . The amount of charges transferred from glycine radical to SWCNT is 0.10e, and the binding energy is -35.1 kcal/mol, which indicates that this is indeed an exothermic adsorption. The present result is opposite to that of Mavrandakis et al,⁵ who showed the C-centered glycine radical could not form a stable complex with (8, 0) SWCNT. Our calculation demonstrates that when the C-centered radical interacts with (8, 0) SWCNT, it undergoes a chemisorption process and could form a quite stable complex with (8, 0) SWCNT.

To interpret this different insight, the HOMO and LUMO of the cluster $C_{64}H_{16}$ employed there are provided in the supporting material, Figure S2. According to Figure S2, it is found that both the HOMO and LUMO of the cluster model distribute at the ends of tube, rather than in the sidewall of the tube as shown in Figure 5 for the extended system. That implies that for the cluster model the active sites probably lie in the ends of tube. If the interaction between molecules/radicals on the sidewall and tube is not quite significantly, that may not be even qualitatively displayed. After study on H_2 adsorption on the finite and infinite nanotubes, a very recent publication concluded that the end of the tube is the most reactive site of all,³² which also basically implies that the ends of nano cluster are more active than the sidewall.

In order to investigate the dependence of the interaction between the C-centered radical and CNT, the periodic DFT with a super cell of 64 carbons is extended to the cells with 96, 128 and 160 carbons. Table 2 shows a slow convergence of the binding energy with the size of the super cell. The interaction becomes stronger by 0.9 kcal/mol from C-64 to C-96, and only 0.5 kcal/mol from C-128 to C-160. Thus, for periodic DFT because of employed 1-dimensional periodic condition the interaction does not significantly change.

It is shown that the C-centered radical **III** is thermodynamically favored over the N-centered radical **IV** by 25.7 kcal/mol. However, when the N-centered radical interacts with (8, 0) SWCNT, the binding of the generated complex **6f** is stronger than system 6e (E_b : -41.4 vs -35.1 kcal/mol), which agrees with the cluster result, where the binding energy between N-radical and (8,0) cluster is -20.2 kcal/mol and +3.5 kcal/mol for C-radical and the cluster⁵. According to Figure 6, in the complex **6e** C-centered radical spreads over the surface, while

N-centered radical sits above the surface in **6f**. The configuration **6f** also undergoes a less significantly deformation, which is evidenced by much smaller deformation energy than **6e** (27.4 vs 44.8 kcal/mol). When the α carbon in the C-centered radical interacts with the surface of SWCNT, because of the strong stereochemical repulsion, the backbone of the C-centered radical undergoes a significant torsion. In the N-centered case, only the NH group was close to the surface of SWCNT and the strong repulsion was therefore avoided. The variation with the super cell sizes of the binding for the N-radical to SWCNT is also collected in Table 2. It seems that the binding energy of the N-radical with the (8,0) converges faster than the C-radical. The binding energy becomes 2.0kcal/mol from C-64 to C-96, yet only 0.5 kcal/mol from C-96 to C-128.

Four configurations are considered of glycine radicals on the surface of B-doped (8, 0) SWCNT, as shown on Figure 7. Figures **7g** and **7i** are the configurations where the C and N atoms of the radicals are bonded to the doped B atom in tube surface, respectively; while Figure **7h** and **7j** show the configurations where the center of radicals are bonded to the C4 atoms in the tube surface. The equilibrium distances, binding energies and the amount of charge transferred from glycine radicals to B-doped SWCNT are listed in Table 2. The calculated binding energies indicate that the doped B atom could promote the adsorption process of glycine radicals on SWCNTs, no matter whether B atom or C4 atom serves as the adsorption site. When the C-centered radical interacts with the B-doped SWCNT, the two different adsorption configurations (**7g** and **7h**) have larger difference in binding energies (-43.1 vs -63.9 kcal/mol) than the configurations **7i** and **7j** (-63.7 vs. -67.2 kcal/mol) resulted from the N-centered radical.

To understand better the reactivity with respect to radical attack in the glycine radicals involved in the adsorption process, their Fukui functions were calculated and shown in Figure 8. The Fukui functions measure the sensitivity of the charge density, $\rho(r)$, with respect to the loss or gain of electrons via the expression²⁶

$$f(r) = (\partial\rho(r)/\partial N)_{v(r)}$$

It can be evaluated for nucleophilic ($f^+(r)$), electrophilic ($f^-(r)$), and radical attack ($f^0(r)$), respectively. A higher value means a greater susceptibility to attack.

As shown in Figure 8c, in the B-doped SWCNT the C4 and B atoms are likely to compete with each other when they interact with radicals. From the viewpoint of electrons, when the B atom replaces the C1 in SWCNT, an electronic hole comes into the electronic structure, thus the B atom plays a role of an electronic acceptor. This electronic acceptor could serve as a target for radical attack. As for C2, C3 and C4 connected to the B atom in B-doped SWCNT, this doping breaks the regular conjugated π system over the central six-membered ring. The p electron of C atom is partly isolated from others, and the C atom could serve as another target for radical attack. The binding energies shown in Table 2 indicate that the radicals, both C-centered and N-centered, were proven to preferentially adsorb on C4 than on B atom (E_b : -63.9 vs -43.1 for **7h** and **7g**; -67.2 vs. -63.7 for **7j** and **7i**). This result reveals that the single electron in p orbital of C atom, perpendicular to the tube surface, has greater sensitivity to glycine radicals.

Figures 8a and 8b show the contour plots of the radical Fukui functions for the C-centered and N-centered radicals. It can be found from Figure 8a that in the C-centered radical, the O atom in carbonyl shows the highest contribution of $f^0(r)$, instead of the α -C. In the case of Figure 8b, the N atom shows the highest contribution of $f^0(r)$. That may be the reason why the complexes formed by the C-centered radical and the two kinds of CNTs are weaker than those formed by the N-centered radicals (E_b : -63.7 vs -43.1 kcal/mol for **7i** and **7g**; -67.2 vs. -63.9 kcal/mol for

7j and **7h**). In the C-centered glycine radical, α -C, located in between N and O, has lower electronegativity than N atom and O atoms. As a result, the single electron therefore was “shared” by the other two electronegative atoms, which is supported by the spin density distribution in Figure 9a. As for the N-centered glycine radical, N atom located far from O atoms, so the single electron was almost “occupied” by itself only as seen in Figure 9b.

3.3 Encapsulation of glycine molecule isomers within the intrinsic (8, 0) SWCNTs.

The one-dimensional structures of glycine encapsulated in intrinsic (8, 0) SWCNT (glycine@ (8, 0)) are discussed in this section. As shown in Figure 11, when a glycine molecule encapsulates into the (8, 0) SWCNT, both SWCNT and the molecules deform significantly. This deformation indicates that the diameter of (8, 0) SWCNT (6.26 Å) is insufficient to hold the molecule. The binding energies for encapsulation process of conformers **I** and **II** are 70.9 and 73.1 kcal/mol, respectively. This means that these encapsulations are endothermic processes and thermodynamically unfavorable at 0K, at which the energetic data are calculated. The encapsulation of conformer **I** into other zigzag SWCNTs, such as (9, 0) and (10, 0) SWCNT is also investigated (Figure 11) and binding energies are plotted in Figure 12. In the case of (9, 0), although the situation is much improved over (8,0) the SWCNT still deform to some extent with a positive binding energy of approximately 16kcal/mol. However, the binding between glycine conformer I and (10, 0) do result in a negative binding energy, and Figure 11 does show both (10, 0) and glycine remain unchanged. Thus, we argue that the critical diameter of the zigzag nanotube for the encapsulation of glycine molecule is about 7.8 Å, the diameter of (10, 0).

4. Conclusion

The adsorptions of a glycine molecule as well as radicals on the side walls of both intrinsic and boron-doped (B-doped) single-walled (8,0) carbon nanotubes (SWCNTs) were investigated by a density functional theory. A glycine molecule tends to physically adsorb on intrinsic SWCNT, yet chemically adsorb on B-doped SWCNT as a result of a somewhat chemical bond between the electron-rich nitrogen atom of the glycine molecule and the electron-scarce boron atom of the doped SWCNT. Opposite to the previous report (*J. Phys. Chem. B* **2006**, *110*, 6048-6050), it is found in the present study that both the N-centered and C-centered glycine radicals can form quite stable complexes with intrinsic as well as B-doped (8, 0) SWCNTs. When the B-doped SWCNT interacts with glycine radicals, although there is a competition between B and the neighbor C in the nanotube axis direction, glycine radicals preferentially bind to the C site. The encapsulations of a glycine molecule into SWCNTs with various diameters are also discussed. We find that the encapsulation process is endothermic for (8, 0) and (9, 0) SWCNTs, while it is exothermic for (10,0) SWCNT, indicating that the critical diameter of the zigzag SWCNT for the encapsulation is 7.83 Å.

Supplementary Material

Refer to Web version on PubMed Central for supplementary material.

Acknowledgment

This work at Shandong University (Sun and Bu) is supported by NSFC (20633060, 20573063), NCET, sdNSF (Z2003B01). The project described was also partially supported by Grant Number SC3GM082324 (Wang's contribution at Albany State University) from the National Institute of General Medical Sciences. The content is solely the responsibility of the authors and does not necessarily represent the official views of the National Institute of General Medical Sciences or the National Institutes of Health.

References

- (1). Iijima S. Helical microtubules of graphitic carbon. *Nature* 1991;354:56–58.
- (2). de Heer WA, Chatelain A, Ugarte D. A Carbon Nanotube Field-Emission Electron Source. *Science* 1995;270:1179–1180.
- (3). Jonge, N. d.; Lamy, Y.; Schoots, K.; Oosterkamp, TH. High brightness electron beam from a multi-walled carbon nanotube. *Nature* 2002;420:393–395. [PubMed: 12459778]
- (4). Hansma PK, Cleveland JP, Radmacher M, Walters DA, Hillner PE, Bezanilla M, Fritz M, Vie D, Hansma HG, Prater CB, Massie J, Fukunaga L, Gurley J, Elings V. Tapping mode atomic force microscopy in liquids. *Appl. Phys. Lett* 1994;64:1738–1740.
- (5). Mavrandakis A, Farantos SC, Froudakis GE. Glycine Interaction with Carbon Nanotubes: An ab Initio Study. *J. Phys. Chem. B* 2006;110:6048–6050. [PubMed: 16553415]
- (6). Wang Y, Bu Y. Noncovalent Interactions between Cytosine and SWCNT: Curvature Dependence of Complexes via $\pi\cdots\pi$ Stacking and Cooperative CH $\cdots\pi$ /NH $\cdots\pi$. *J. Phys. Chem. B* 2007;111:6520–6526. [PubMed: 17508735]
- (7). Singh R, Pantarotto D, McCarthy D, Chaloin O, Hoebeke J, Partidos CD, Briand J-P, Prato M, Bianco A, Kostarelos K. Binding and Condensation of Plasmid DNA onto Functionalized Carbon Nanotubes: Toward the Construction of Nanotube-Based Gene Delivery Vectors. *J. Am. Chem. Soc* 2005;127:4388. [PubMed: 15783221]
- (8). Bianco A, Kostarelos K, Partidos CD, Prato M. Biomedical applications of functionalised carbon nanotubes. *Chem. Commun* 2005;5:571–577.
- (9). Bianco A, Kostarelos K, Prato M. Applications of carbon nanotubes in drug delivery. *Curr. Opin. Chem. Biol* 2005;9:674–679. [PubMed: 16233988]
- (10). Lin Y, Lu F, Tu Y, Ren Z. Glucose Biosensors Based on Carbon Nanotube Nanoelectrode Ensembles. *Nano Lett* 2004;4:191–195.
- (11). Zhao Q, Buongiorno Nardelli M, Lu W, Bernholc J. Carbon Nanotube-Metal Cluster Composites: A New Road to Chemical Sensors? *Nano Lett* 2005;5:847–851. [PubMed: 15884882]
- (12). Wang J. Carbon-Nanotube Based Electrochemical Biosensors: A Review. *Electroanalysis* 2005;17:7–14.
- (13). Davis JJ, Green MLH, Hill HAO, Leung YC, Sadler PJ, Sloan J, Xavier AV, Tsang SC. The immobilisation of proteins in carbon nanotubes. *Inorg. Chim. Acta* 1998;272:261–266.
- (14). Balavoine F, Schultz P, Richard C, Mallouh V, Ebbesen TW, Mioskowski C. Helical Crystallization of Proteins on Carbon Nanotubes: A First Step towards the Development of New Biosensors. *Angew. Chem. Int. Ed* 1999;38:1912.
- (15). Bianco A, Prato M. Can Carbon Nanotubes be Considered Useful Tools for Biological Applications? *Adv. Mater* 2003;15:1765–1768.
- (16). Pantarotto D, Partidos CD, Graff R, Hoebeke J, Briand J-P, Pratto M, Bianco A. Synthesis, Structural Characterization, and Immunological Properties of Carbon Nanotubes Functionalized with Peptides. *J. Am. Chem. Soc* 2003;125:6160–6164. [PubMed: 12785847]
- (17). Peng S, Cho K. Ab Initio Study of Doped Carbon Nanotube Sensors. *Nano Lett* 2003;3:513–517.
- (18). Wang R, Zhang D, Zhang Y, Liu C. Boron-Doped Carbon Nanotubes Serving as a Novel Chemical Sensor for Formaldehyde. *J. Phys. Chem. B* 2006;110:18267–18271. [PubMed: 16970445]
- (19). Zhang YM, Zhang DJ, Liu CB. Novel Chemical Sensor for Cyanides: Boron-Doped Carbon Nanotubes. *J. Phys. Chem. B* 2006;110:4671–4674. [PubMed: 16526700]
- (20). Perdew JP, Wang Y. Accurate and simple analytic representation of the electron-gas correlation energy. *Phys. Rev. B* 1992;45:13244–13249.
- (21). Srivastva D, Menon M, Cho K. Nanoplasticity of Single-Wall Carbon Nanotubes under Uniaxial Compression. *Phys. Rev. Lett* 1999;83:2973–2976.
- (22). Frisch, MJ.; Trucks, GW.; Schlegel, HB.; Scuseria, GE.; Robb, MA.; Cheeseman, JR.; Montgomery, JA., Jr.; Vreven, T.; Kudin, KN.; Burant, JC.; Millam, JM.; Iyengar, SS.; Tomasi, J.; Barone, V.; Mennucci, B.; Cossi, M.; Scalmani, G.; Rega, N.; Petersson, GA.; Nakatsuji, H.; Hada, M.; Ehara, M.; Toyota, K.; Fukuda, R.; Hasegawa, J.; Ishida, M.; Nakajima, T.; Honda, Y.; Kitao, O.; Nakai, H.; Klene, M.; Li, X.; Knox, JE.; Hratchian, HP.; Cross, JB.; Bakken, V.; Adamo, C.; Jaramillo, J.; Gomperts, R.; Stratmann, RE.; Yazyev, O.; Austin, AJ.; Cammi, R.; Pomelli, C.; Ochterski, JW.;

- Ayala, PY.; Morokuma, K.; Voth, GA.; Salvador, P.; Dannenberg, JJ.; Zakrzewski, VG.; Dapprich, S.; Daniels, AD.; Strain, MC.; Farkas, O.; Malick, DK.; Rabuck, AD.; Raghavachari, K.; Foresman, JB.; Ortiz, JV.; Cui, Q.; Baboul, AG.; Clifford, S.; Cioslowski, J.; Stefanov, BB.; Liu, G.; Liashenko, A.; Piskorz, P.; Komaromi, I.; Martin, RL.; Fox, DJ.; Keith, T.; Al-Laham, MA.; Peng, CY.; Nanayakkara, A.; Challacombe, M.; Gill, PMW.; Johnson, B.; Chen, W.; Wong, MW.; Gonzalez, C.; Pople, JA. Gaussian 03, Revision D.01. Gaussian, Inc.; Wallingford CT: 2004.
- (23). Saito, R.; Dresselhaus, G.; Dresselhaus, MS. Physical Properties of Carbon Nanotubes. Imperial College Press; London, UK: 2001.
- (24). Bauschlicher CW Jr. Ricaca A. Binding of NH₃ to graphite and to a (9, 0) carbon nanotube. *Phys. Rev. B* 2004;70:115409.
- (25). Wu X, An W, Zeng XC. Chemical Functionalization of Boron-Nitride Nanotubes with NH₃ and Amino Functional Groups. *J. Am. Chem. Soc* 2006;128:12001–12006. [PubMed: 16953642]
- (26). Parr R,G, Yang WT. Density functional approach to the frontier-electron theory of chemical reactivity. *J. Am. Chem. Soc* 1984;106:4049–4050.
- (27). Attila G. Conformers of gaseous glycine. *J. Am. Chem. Soc* 1992;114:9568–9575.
- (28). (a) Delley B. An all-electron numerical method for solving the local density functional for polyatomic molecules. *J. Chem. Phys* 1990;508–517. (b) Delley B. From molecules to solids with the DMol³ approach. *J. Chem. Phys* 2000;113:7756–7764.
- (29). Yu D, Rauk A, Armstrong DA. Radicals and Ions of Glycine: An ab Initio Study of the Structures and Gas-Phase Thermochemistry. *J. Am. Chem. Soc* 1995;117:1789–1796.
- (30). Huang Y, Guler L, Heidbrink J, Kenttaemaa H. Reactions of Charged Phenyl Radicals with Aliphatic Amino Acids in the Gas Phase. *J. Am. Chem. Soc* 1995;117:1789–1796.
- (31). Wang YX, Balbuena PB. Associations of Alkyl Carbonates: Intermolecular C-H···O Interactions. *J. Phys. Chem. A* 2001;105:9972–9982.
- (32). Bilic A, Gale JD. Chemisorption of Molecular Hydrogen on Carbon Nanotubes: A Route to Effective Hydrogen Storage? *J. Phys. Chem. C*. 2008ASAP

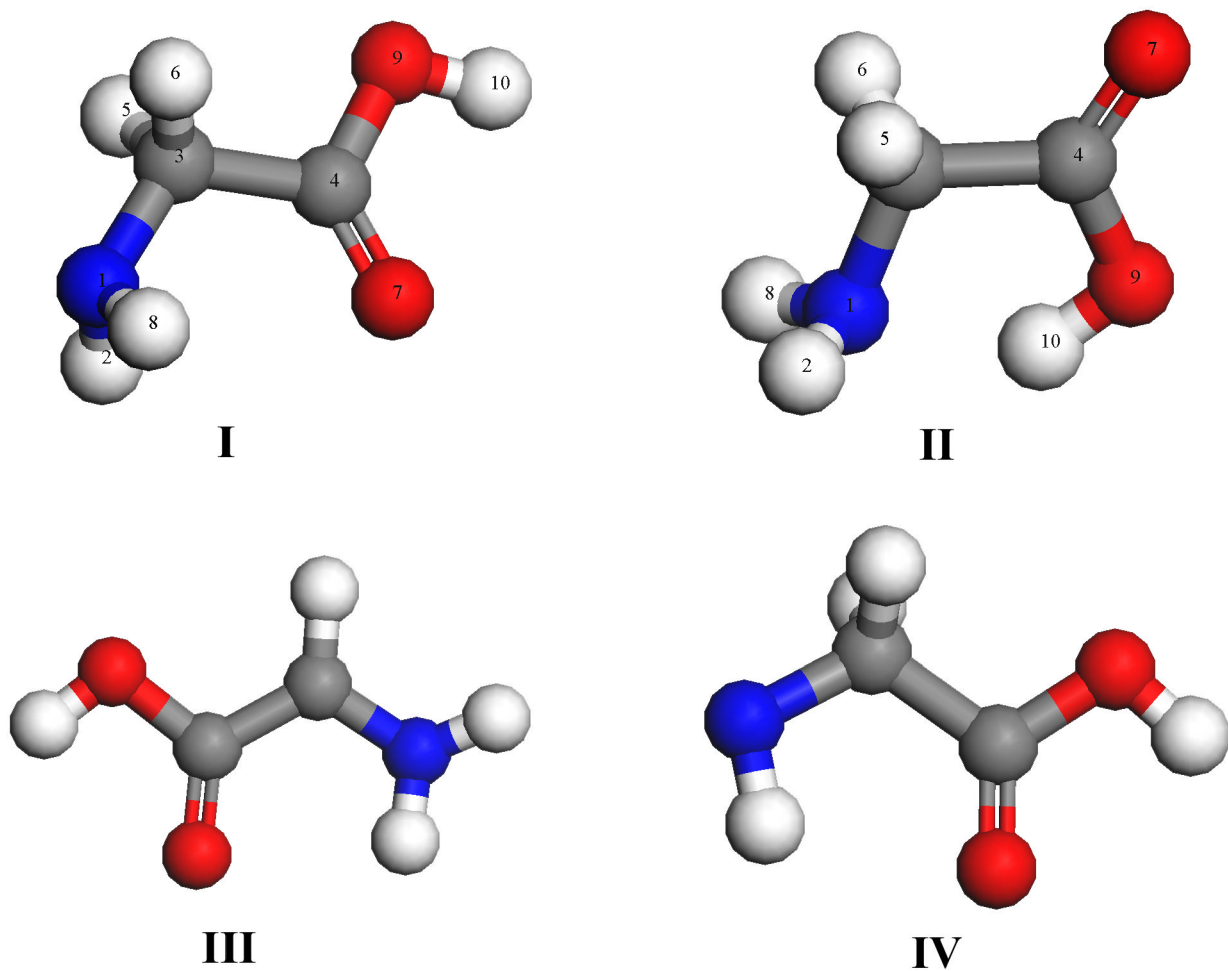
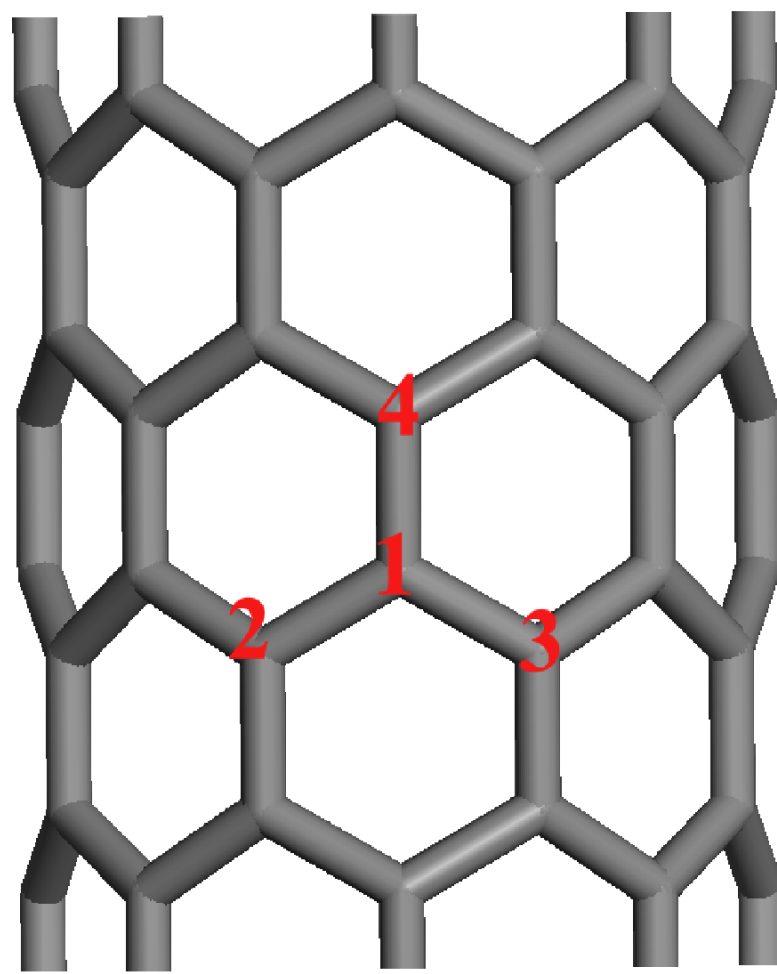


Figure 1.
Optimized structures for glycine molecules and glycine radicals.

**Figure 2.**

Structural model of the (8, 0) SWCNT, where the carbon atom in site 1 will be replaced by a B atom to model a B-doped SWCNT and the sites 2, 3, and 4 are the carbon atoms near the doped B atom.

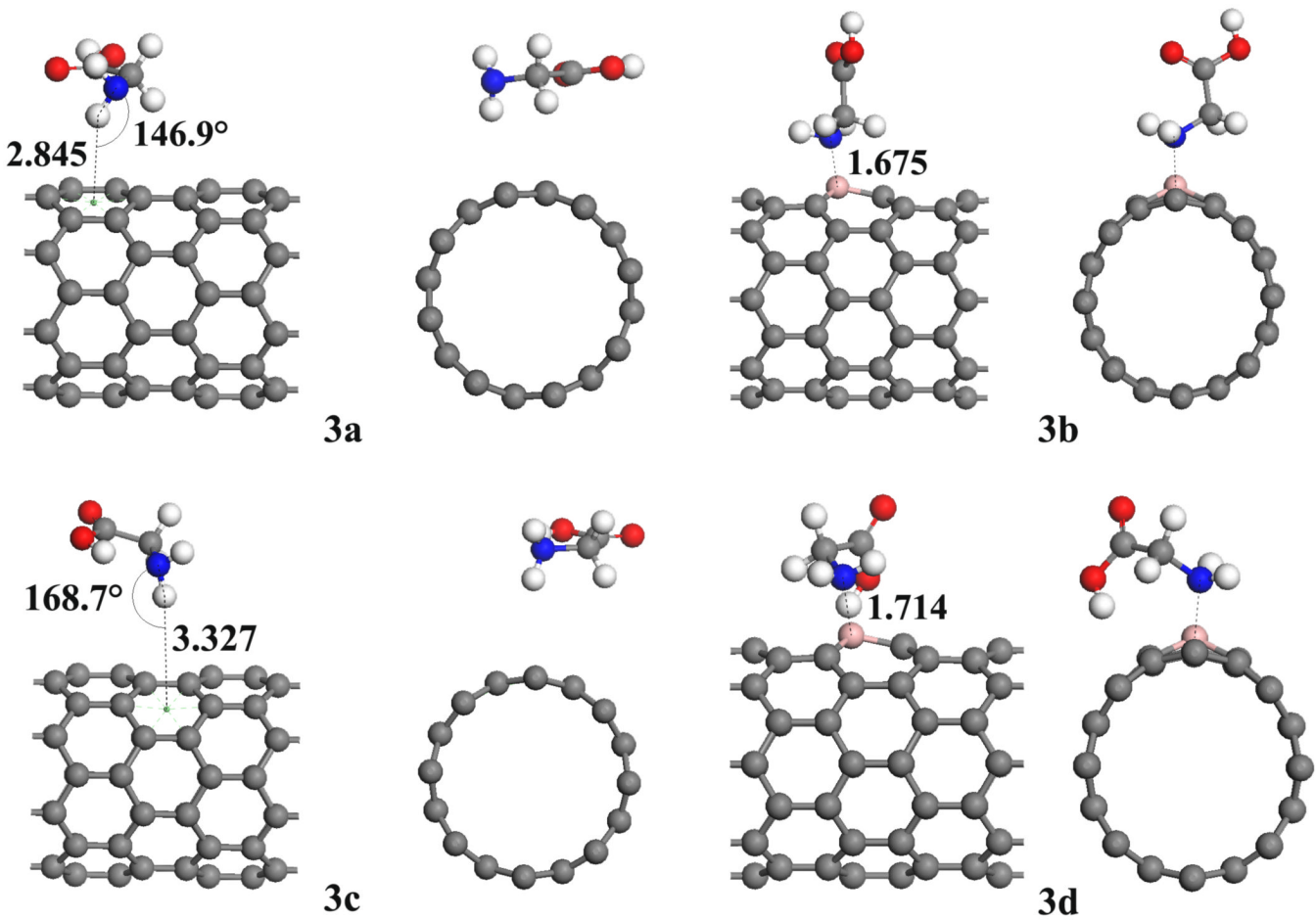
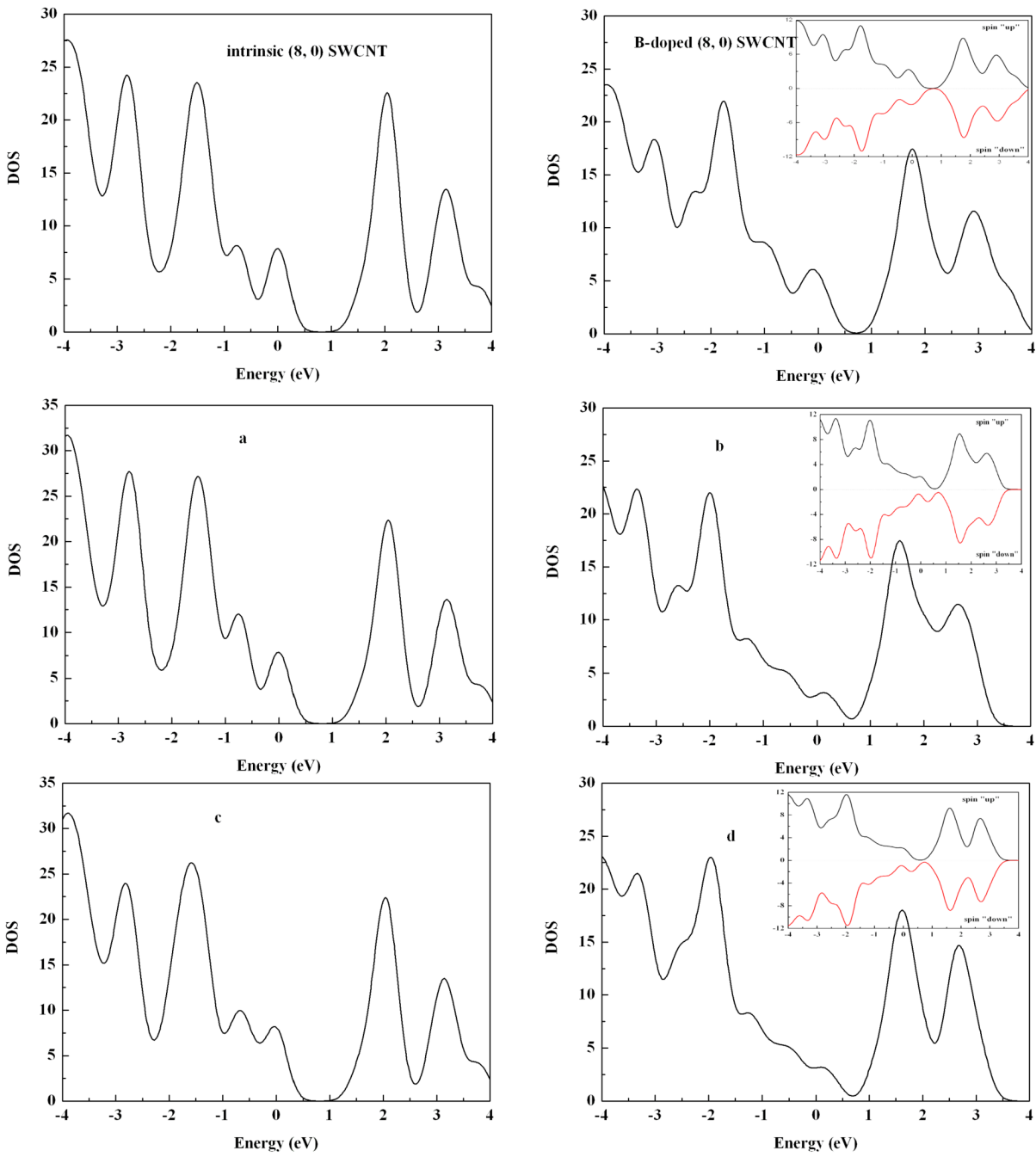


Figure 3.
Optimized configurations for the complexes (3a) glycine molecule **I** on intrinsic (8, 0) SWCNT,
(3b) glycine molecule **I** on B-doped (8, 0) SWCNT, (3c) glycine molecule **II** on intrinsic (8,
0) SWCNT and (3d) glycine molecule **II** on B-doped (8, 0) SWCNT.

**Figure 4.**

Total DOS graphs for the intrinsic (8, 0) SWCNT, B-doped (8, 0) SWCNT, the complex I-SWCNT (**a**), I-B-doped SWCNT (**b**), II-SWCNT (**c**) and II-B-doped SWCNT (**d**). The inserted pictures in **b** and **d** are the corresponding spin-up and spin-down DOSs.

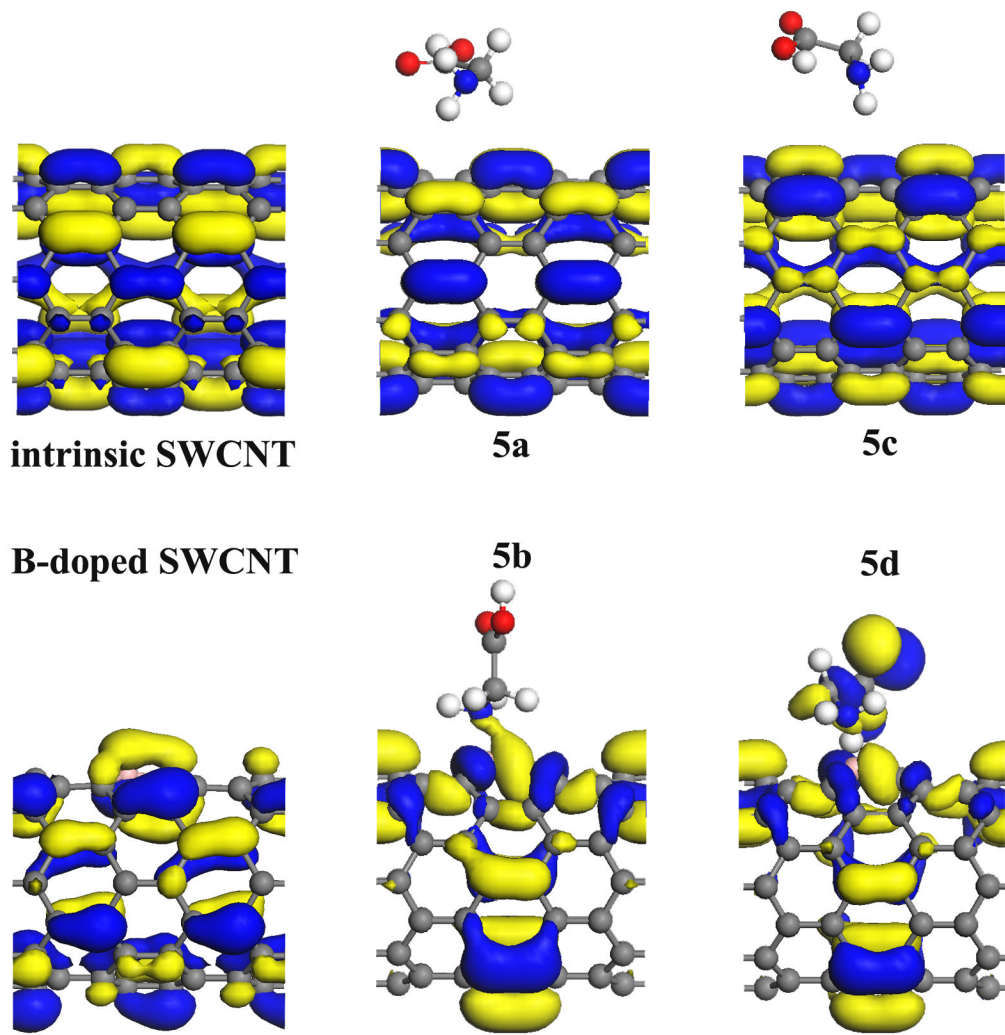


Figure 5.
HOMOs of intrinsic (8, 0) SWCNT, B-doped (8, 0) SWCNT, the complex I-SWCNT (5a) and II-SWCNT (5c). Graphs of 5b and 5d show the isosurfaces of the B-N bonds in I-B-doped SWCNT and II-B-doped SWCNT, respectively.

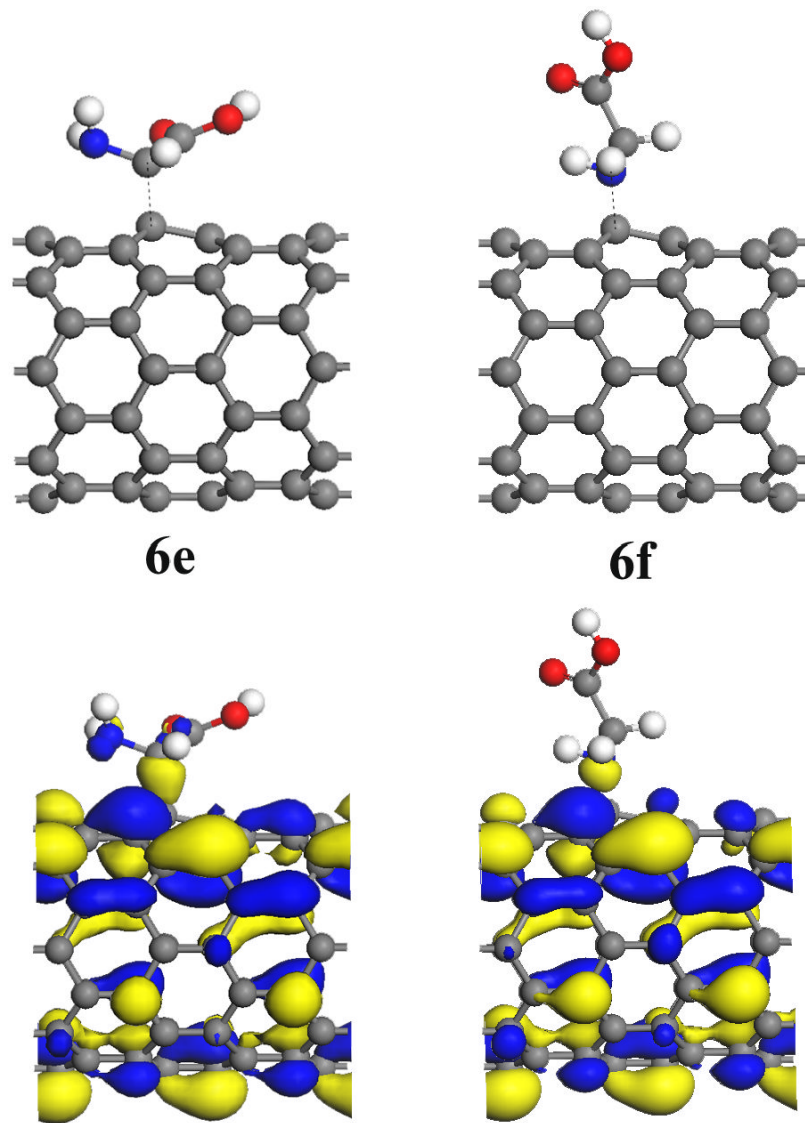
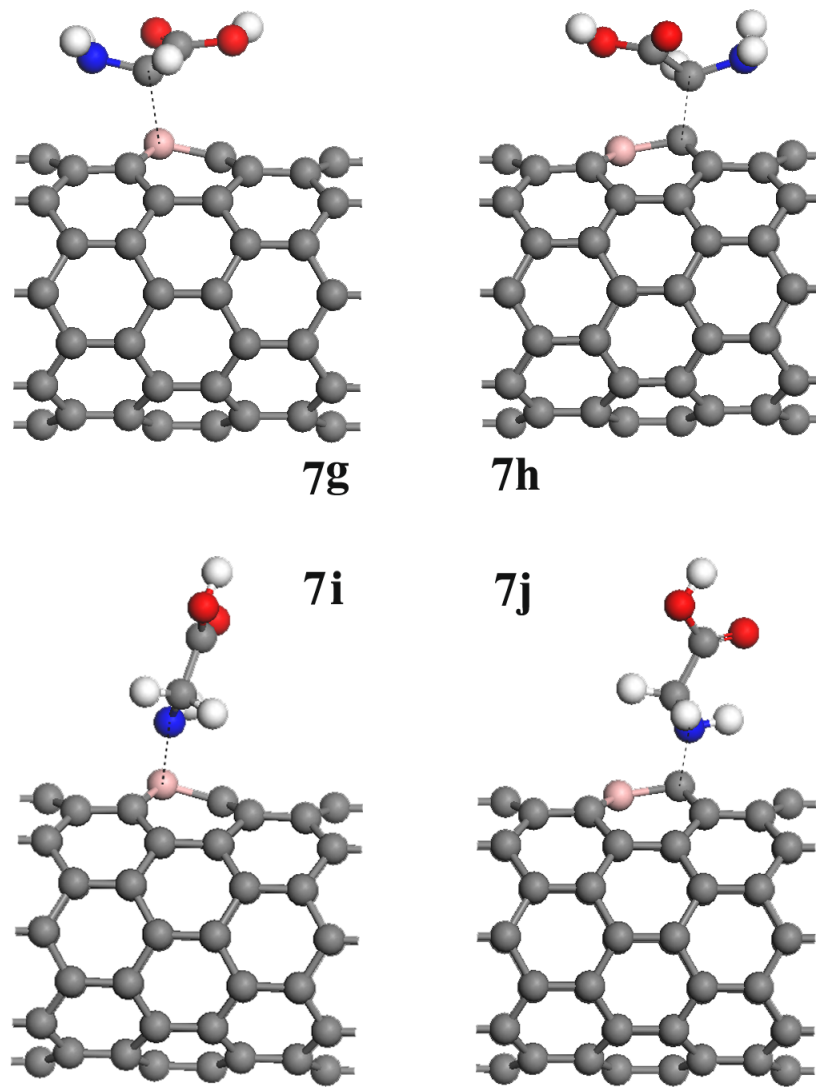


Figure 6.

Optimized structures and HOMO graphs for the C-centered-radical bonded to the intrinsic (8, 0) SWCNT (**6e**), and for the N-centered-radical bonded to the intrinsic (8, 0) SWCNT (**6f**).

**Figure 7.**

The optimized geometry of the complex: the C-centered radical bonded to the B atom (**7g**), the C-centered radical bonded to the C atom (**7h**), the N-centered radical bonded to the B atom (**7i**), and the N-centered radical bonded to the B atom (**7j**).

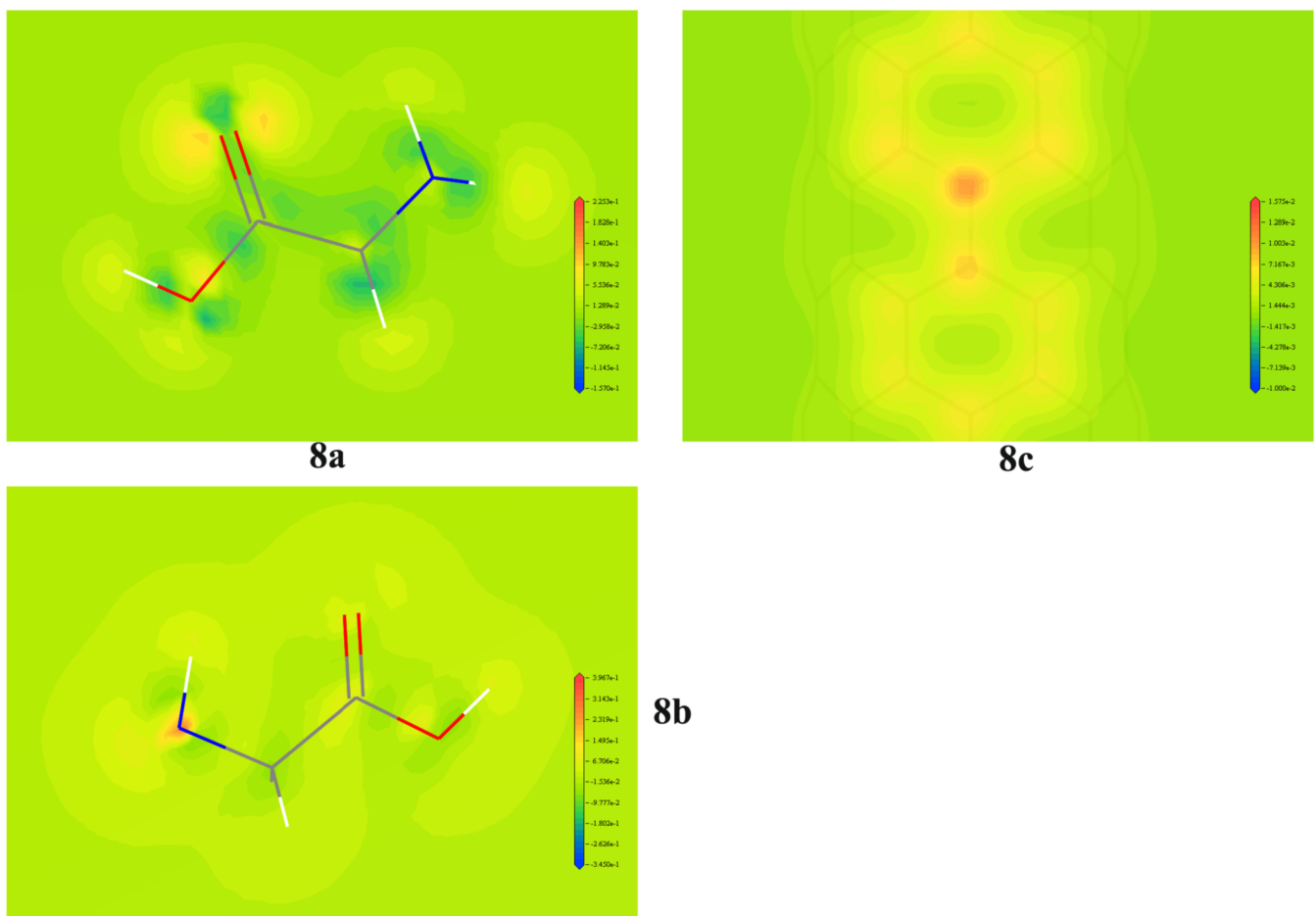


Figure 8.

Contour plot of the radical Fukui functions of C-centered radical (**8a**), N-centered radical (**8b**) and B-doped SWCNT (**8c**). The highest and lowest values are indicated in the scale by the red and blue colors, respectively. The blue, gray, white and pink lines indicate the nitrogen, carbon, hydrogen and boron atoms, respectively.

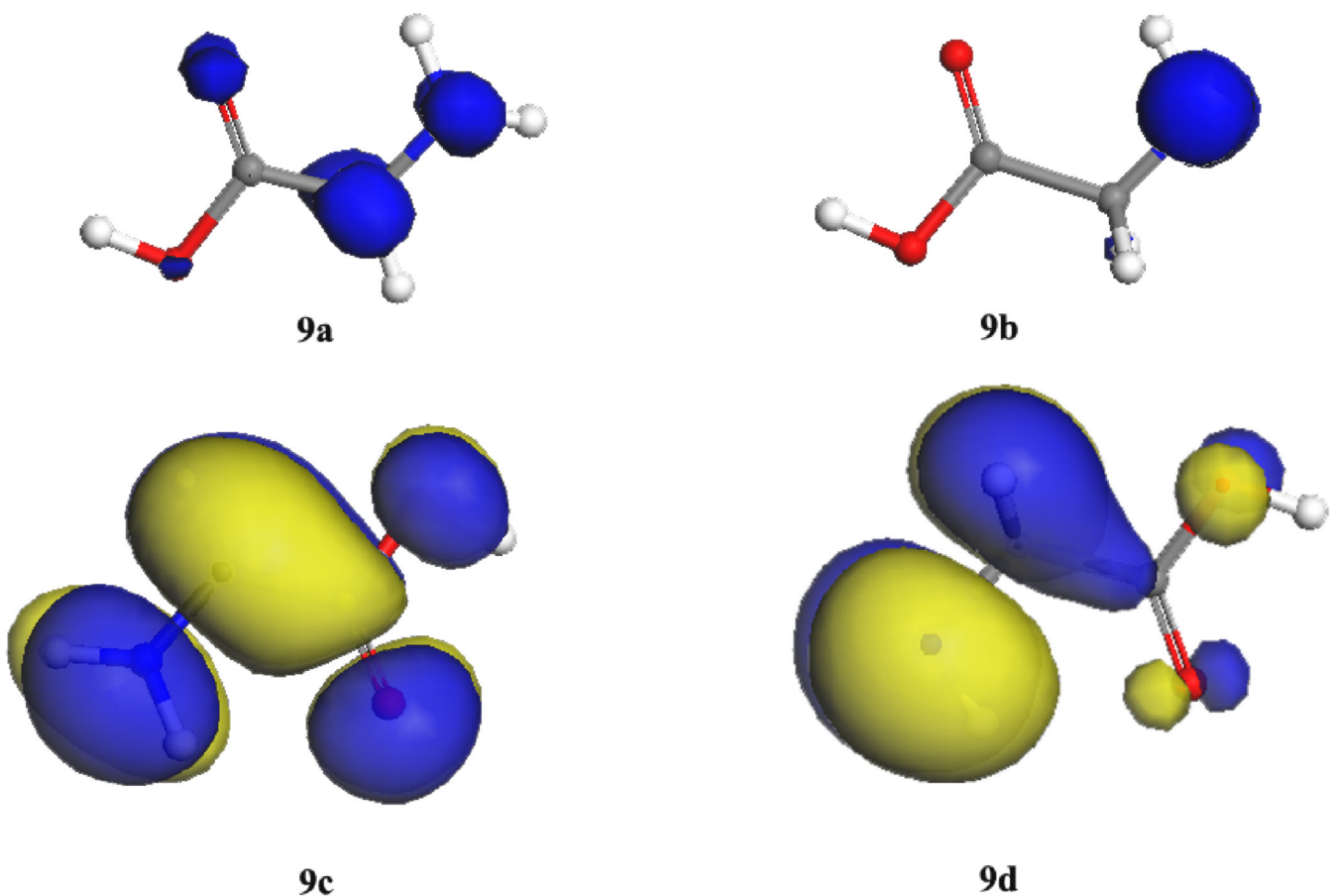


Figure 9.

Isodensity surfaces of the spin electronic density for the C-centered glycine radical (9a) and the N-centered radical (9b) with isosurface values of 0.2. The HOMOs of the C-centered radical (9c) and the N-centered radical (9d) with isosurface values of 0.02.

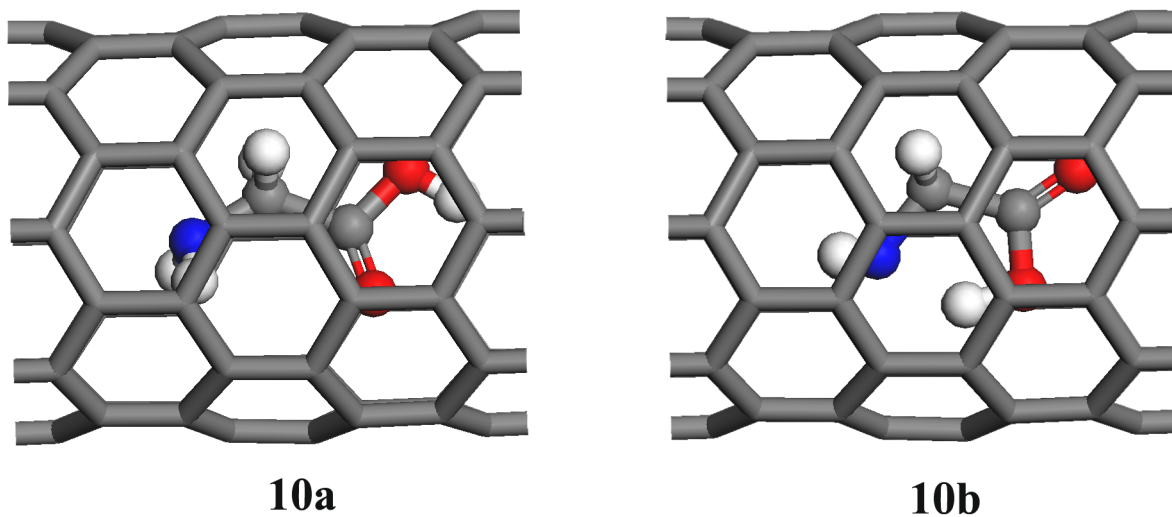


Figure 10.

Optimized geometries of glycine molecule **I** (a) and **II** (b) in intrinsic (8, 0) SWCNT.

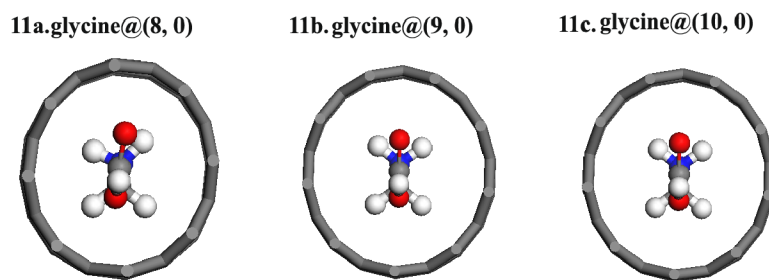


Figure 11.

Optimized geometries of glycine molecule in (a) (8, 0), (b) (9, 0) and (10, 0) SWCNTs.

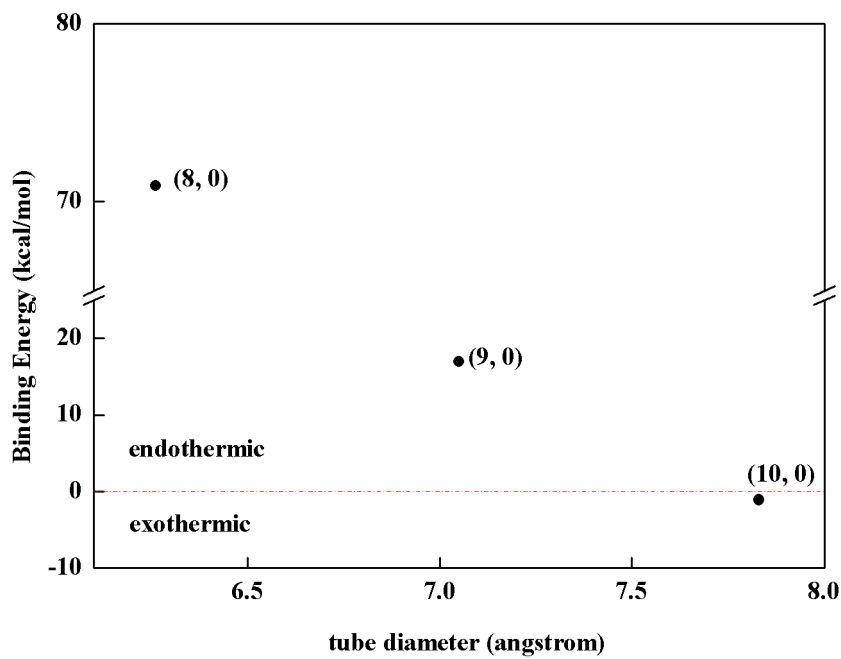


Figure 12.

Binding energies E_b per glycine molecule in the encapsulation process for the (8, 0), (9, 0), and (10, 0) SWCNTs. A simple linear interpolation shows that the binding energy crosses zero at the tube diameter of 7.78 Å.

Table 1

The HOMO-LUMO gap (eV), binding energy (E_b , kcal/mol), and amount charge (q/e) for the complexes resulting from the adsorptions of glycine molecule isomers on SWCNT and B-doped (8,0) SWCNT.

Configuration ^a	Gap ^b	E_b	q ^c
3a: I+(8,0)	0.61	-1.4	-0.01
3c: II+(8,0)	0.60	-1.6	-0.01
3b:I+B-(8,0)	0.24	-33.2	0.32
3d:II+B-(8,0)	0.18	-33.9	0.29

^a all the configurations were given in Figure 3.

^b HOMO-LUMO energy gap calculated using Γ point.

^c The amount of charges transferred from glycine molecules to intrinsic or B-doped SWCNT

Table 2
Equilibrium distances (d/Å), binding energy (E_b , kcal/mol) and charge transfer (q/e) for various configurations resulting from the glycine radicals (III and IV) and (8,0) SWCNT.

Configuration ^c	d ^a	E_b	q ^b
6e: III+64-(8,0)	1.629	-35.1	0.10
III+96-(8,0)	1.637	-36.0	0.13
III+128-(8,0)	1.636	-36.8	0.13
IV+160-(8,0)	1.635	-37.3	0.13
6f: IV+64-(8,0)	1.484	-41.4	0.07
IV+96-(8,0)	1.484	-43.4	-0.03
IV+128-(8,0)	1.484	-43.9	-0.03
7g:III+B-doped (8,0), C-B	1.814	-43.1	0.16
7h:III+ B-doped (8,0), C-C	1.613	-63.9	0.11
7i:IV+ B-doped (8,0), N-B	1.555	-63.7	0.13
7j:IV+ B-doped (8,0), N-C	1.484	-67.2	0.09

^athe distances between radical center and adsorption site.

^bThe amount of charges transferred from glycine radicals to intrinsic or B-doped SWCNT.

^cthe configurations are given in Figures 6 and 7; 64-(8,0) refers to the cell size of 64 carbons and so on.